

# Exact decoherence dynamics of $1/f$ noise

Md. Manirul Ali,<sup>1,\*</sup> Ping-Yuan Lo,<sup>1</sup> and Wei-Min Zhang<sup>1,†</sup>

<sup>1</sup>*Department of Physics, National Cheng Kung University, Tainan 70101, Taiwan*

(Dated: October 7, 2014)

In this paper, we investigate the exact decoherence dynamics of a superconducting resonator coupled to an electromagnetic reservoir characterized by the  $1/f$  noise at finite temperature, where a full quantum description of the environment with  $1/f^x$  noise (with  $x \approx 1$ ) is presented. The exact master equation and the associated nonequilibrium Green's functions are solved exactly for such an open system. We show a clear signal of non-Markovian dynamics induced purely by  $1/f$  noise. Our analysis is also applicable to another nano/micro mechanical oscillators. Finally, we demonstrate the non-Markovian decoherence dynamics of photon number superposition states using Wigner distribution that could be measured in experiments.

PACS numbers: 03.65.Yz, 03.67.Pp, 42.50.Lc, 03.65.Ta

Keywords:  $1/f$  noise, exact decoherence, non-Markovian dynamics

## I. INTRODUCTION

Low frequency noise spectrum  $S(f) \sim 1/f$  was discovered in vacuum tubes and later observed in a variety of systems [1–4]. In electronics, this type of noise is commonly referred to as  $1/f$  noise. Miniaturization of any material system in nanometer-scale devices can further increase  $1/f$  noise levels and complicate practical applications [5, 6]. The sensitivity of amplifiers and transducers used in many types of sensor, particularly those that rely on an electrical response, is ultimately limited by the low-frequency noise level [7, 8]. The importance of  $1/f$  noise in electronics has motivated various studies of its physical mechanisms and the development of a variety of methods for its reduction [6]. Different physical origin of fluctuation processes can be responsible for the  $1/f$  noise in different materials and devices [9–11].

In almost all quantum computing nanodevices,  $1/f$  noise is found to be detrimental to the required maintenance of quantum coherent dynamics. In the last two decades, several experiments with single electron transistors (SETs) [12–16] and superconducting circuits [17–23] at low temperatures revealed low-frequency noise with a spectrum that scales inversely with frequency ( $1/f$ ). The models and experimental observations [26–32] suggest that the proper scaling of this low frequency noise should be  $1/f^x$  where  $x$  may differ slightly from unity. We will investigate the exact decoherence dynamics of a superconducting resonator in presence of this noise with varying values of  $x$ , including the situation under  $1/f$  noise where  $x \rightarrow 1$ . Our analysis is also applicable to other nanomechanical oscillators. Superconducting resonators and nano/micro mechanical oscillators have achieved sufficiently high frequencies (GHz range), and work at very low temperature (mK range), in which nonclassical photon states can be rather easily generated [37–39]. Recently,  $1/f$  noise is measured both in superconducting

resonator [40, 41] as well as in the mechanical oscillator [42, 43].

Usually, in the literature on  $1/f$  noise, the environment is treated classically as a random field describing a stochastic process [27–32]. We investigate in this paper the exact decoherence dynamics of a superconducting resonator coupled to an electromagnetic reservoir characterized by the  $1/f$  frequency noise, where a full quantum description of the environment with  $1/f$  noise is presented. We also describe the decoherence dynamics of nonclassical photon states of the resonator through the evolution of Wigner distribution function. The paper is organized as follows. In Sec. II, we briefly discuss our model and the method we used. The noise power spectrum is explored in Sec. III in the exact formalism of the nonequilibrium Green's functions. In Sec. IV, we present our numerical results on the exact decoherence dynamics of  $1/f^x$  noise at finite temperature through the exact solution of the master equation associated with the nonequilibrium Green's functions. Using Wigner distribution, we demonstrate in Sec. V the exact decoherence dynamics of superposition of photon number states under  $1/f^x$  noise with different values of  $x$ . Finally, a conclusion is given in Sec. VI.

## II. THE MODEL AND THE EXACT MASTER EQUATION

We consider a superconducting or a nanomechanical resonator coupled to an electromagnetic reservoir, the Hamiltonian of the total system can be written as

$$H = \hbar\omega_0 a^\dagger a + \sum_k \hbar\omega_k b_k^\dagger b_k + \sum_k \hbar \left( V_k a^\dagger b_k + V_k^* a b_k^\dagger \right) \mathbf{1}$$

where the first term is the Hamiltonian  $H_S$  of the single-mode resonator with frequency  $\omega_0$ , and  $a^\dagger$  and  $a$  are the creation and annihilation operators of the resonator quanta; the second term is the Hamiltonian  $H_E$  of a general electromagnetic reservoir, as a collection of infinite

\* mani@mail.ncku.edu.tw

† wzhang@mail.ncku.edu.tw

photon or phonon modes, where  $b_k^\dagger$  and  $b_k$  are the corresponding creation and annihilation operators of the  $k$ -th photon or phonon mode with frequency  $\omega_k$ . The third term is the system-reservoir coupling  $H_I$  which characterizes photon scattering processes with the scattering amplitude  $V_k$  between the resonator and the  $k$ -th reservoir mode. The nonlinear photonic processes have been ignored in Eq. (1) because the  $1/f$  noise spectrum only occurs in the very weak-coupling regime between the systems and its environment, as we will show in Sec. III.

We shall use the exact master equation method to describe the decoherence dynamics of the resonator under the influence of the  $1/f$  noise. The master equation is given in terms of the reduced density operator, obtained from the density operator of the total system by tracing over the environmental degrees of freedom  $\rho(t) = \text{Tr}_E[\rho_{tot}(t)]$ . The total density operator is governed by the quantum evolution operator:  $\rho_{tot}(t) = e^{-\frac{i}{\hbar}H(t-t_0)}\rho_{tot}(t_0)e^{\frac{i}{\hbar}H(t-t_0)}$ . As it was originally proposed by Feynman and Vernon [44–47], we take the initial state of the total system as a directly product of an arbitrary initial state of the system with the thermal state of the reservoir,  $\rho_{tot}(t_0) = \rho(t_0) \otimes \rho_E(t_0)$ , where  $\rho_E(t_0) = \exp(-\beta H_E)/\text{Tr}[\exp(-\beta H_E)]$ . In this case, tracing over all the environmental degrees of freedom can be easily carried out using the Feynman-Vernon influence functional approach [44, 45] in the framework of coherent-state path-integral representation [48, 49]. The resulting master equation for the reduced density operator has the following form [49]:

$$\begin{aligned} \frac{d\rho(t)}{dt} = & -i\omega'_0(t) [a^\dagger a, \rho(t)] \\ & + \gamma(t) [2a\rho(t)a^\dagger - a^\dagger a\rho(t) - \rho(t)a^\dagger a] \\ & + \tilde{\gamma}(t) [a\rho(t)a^\dagger + a^\dagger \rho(t)a - a^\dagger a\rho(t) - \rho(t)aa^\dagger], \end{aligned} \quad (2)$$

where the time-dependent coefficient  $\omega'_0(t)$  is the renormalized frequency of the resonator, while  $\gamma(t)$  and  $\tilde{\gamma}(t)$  describe the dissipation (damping) and fluctuation (noise) of the resonator due to its coupling to the reservoir. These coefficients can be exactly determined by the following relations [49–52]

$$\begin{aligned} \omega'_0(t) = & -\text{Im} \left[ \frac{\dot{u}(t)}{u(t)} \right], \quad \gamma(t) = -\text{Re} \left[ \frac{\dot{u}(t)}{u(t)} \right], \\ \tilde{\gamma}(t) = & \dot{v}(t) - 2v(t)\text{Re} \left[ \frac{\dot{u}(t)}{u(t)} \right]. \end{aligned} \quad (3)$$

The function  $u(t)$  is the nonequilibrium propagating (or spectral) Green's function of the system, which satisfies the Dyson equation of motion

$$\dot{u}(t) + i\omega_0 u(t) + \int_{t_0}^t d\tau g(t-\tau)u(\tau) = 0, \quad (4)$$

subject to the initial condition  $u(t_0) = 1$ . The nonequilibrium thermal fluctuation is characterised by the correlation function  $v(t)$  through the nonequilibrium

fluctuation-dissipation theorem [53], which is given explicitly by

$$v(t) = \int_{t_0}^t d\tau \int_{t_0}^t d\tau' \tilde{g}(\tau - \tau') u^*(\tau) u(\tau'). \quad (5)$$

The time correlation functions  $g(t - \tau)$  and  $\tilde{g}(\tau - \tau')$  in Eqs. (4) and (5) are given by

$$g(t - \tau) = \int_0^\infty \frac{d\omega}{2\pi} J(\omega) e^{-i\omega(t-\tau)} \quad (6)$$

$$\tilde{g}(\tau - \tau') = \int_0^\infty \frac{d\omega}{2\pi} J(\omega) \bar{n}(\omega, T) e^{-i\omega(\tau-\tau')} \quad (7)$$

which characterize all the non-Markovian back-action memory effects between the system and the reservoir, where  $J(\omega) = 2\pi \sum_k |V_k|^2 \delta(\omega - \omega_k)$  is the spectral density, and  $V_k$  is the coupling between the system and the reservoir. Furthermore,  $\bar{n}(\omega, T) = \frac{1}{e^{\hbar\omega/k_B T} - 1}$  is the particle number distribution of the bosonic reservoir at the initial temperature  $T$ . If the reservoir spectrum is continuous,  $V_k \rightarrow V(\omega)$ , we have  $J(\omega) = 2\pi \varrho(\omega) |V(\omega)|^2$  where  $\varrho(\omega)$  is the density of state of the reservoir.

### III. QUANTUM DESCRIPTION OF $1/f$ NOISE SPECTRUM

In the literature on  $1/f$  noise, the environment is treated classically [27–32] with a classical random field  $c(t)$  describing a stochastic process. The system-environment coupling is described by a term  $\sim c(t)A$ , and  $A$  is a system operator. Then the system Hamiltonian becomes stochastic due to the random nature of the classical random field  $c(t)$  which can take different form corresponding to different kinds of classical noise. A typical classical noise source is the random telegraphic noise (RTN) which is used to classically model an environment for solid-state devices [11, 31, 32] (and references therein), where the system is considered to be interacting with a bistable fluctuator for which the time-dependent parameter randomly flipping between two values  $c(t) = \pm 1$  with a switching rate  $\nu$ . The Hamiltonian with such a noise source describing a system subject to a random telegraph noise is usually used as a basic building block to describe noises of the type  $1/f^\alpha$ , and is characterized by an exponentially decaying correlation function  $e^{-\nu|t|}$  of the fluctuating quantity  $c(t)$ . Then the noise spectrum is a Lorentzian function

$$\begin{aligned} \mathcal{S}(\omega, \nu) = & \int_{-\infty}^{+\infty} dt e^{i\omega t} \overline{c(t)c(0)} \\ = & \int_{-\infty}^{+\infty} dt e^{i\omega t} e^{-\nu|t|} = \frac{1}{\pi} \frac{\nu}{\omega^2 + \nu^2}. \end{aligned} \quad (8)$$

To reproduce the  $1/f^\alpha$  spectrum, the single RTN frequency power spectrum is then integrated over the

switching rates  $\nu$  with a suitable probability distribution:

$$\mathcal{S}_{1/f^\alpha}(\omega) = \int_{\nu_1}^{\nu_2} \mathcal{S}(\omega, \nu) p_\alpha(\nu) d\nu, \quad (9)$$

The integration is generally performed between a minimum and a maximum value of the switching rates,  $\nu_1$  and  $\nu_2$  respectively. In order to simulate  $1/f^\alpha$  noise spectrum, the switching rate distribution  $p_\alpha(\nu)$  is considered to be proportional to  $1/\nu^\alpha$ . When the integration in Eq.(9) is performed, the spectrum shows  $1/f^\alpha$  behavior in a frequency interval, so that all frequencies belonging to such an interval satisfies the condition  $\nu_1 \leq f \leq \nu_2$ . Although this low and high frequency cutoff frequencies are artificially fixed in the literature [17–19, 21, 24], the physical origin of the cutoff frequencies are debatable [25]. Another crucial point is that the classical environment with the noise spectrum  $1/f^\alpha$  can be realized by different configuration of bistable fluctuators. Noise spectrum  $1/f^\alpha$  can be obtained either considering a single bistable fluctuator whose switching rate is randomly chosen from a distribution  $p_\alpha(\nu)$  as shown above. The same  $1/f^\alpha$  spectrum can also be realized from the coupling of a system with a large number of fluctuators, where the noise spectrum can be obtained as a result of linear combination of many Lorentzian, each characterized by a specific switching rate [11, 31, 32]. As already pointed out in several papers [31, 33–36], different microscopic configuration of the environment leading to the same spectra may correspond to different physical phenomena. Thus, mere knowledge of the noise spectrum is not sufficient to describe the environmental influence on the quantum dynamics of open systems and it is necessary to specify the model for the noise source in more detail.

In the previous section, we have presented a full quantum-mechanical description of the system-environment coupling for a superconducting resonator coupled to an electromagnetic reservoir. Before we explore the decoherence dynamics of a superconducting resonator or a nanomechanical resonator, induced by the  $1/f$  noise, it is important to justify the conditions for the occurrence of  $1/f$  noise in a given electromagnetic reservoir characterized by the spectral density  $J(\omega)$ . In the literature, the spectral density  $J(\omega)$  for an electromagnetic reservoir is found to be Ohmic-type [46], given by

$$J(\omega) = 2\pi\eta \omega \left(\frac{\omega}{\omega_c}\right)^{s-1} e^{-\omega/\omega_c}, \quad (10)$$

with  $0 < x = (1 - s) < 1$ . It has been pointed out [56] that the  $1/f$  noise spectrum corresponds to the special case of the spectral density (10) with  $s \approx 0$  or  $x \approx 1$ . However, the exact connection of  $J(\omega)$  with the noise spectrum  $S(\omega)$  has not been carried out so far in the literature. Here, within the exact master equation formalism, we find that the exact solutions of the nonequilibrium Green's functions  $u(t)$  and  $v(t)$  carry all the information on the quantum nature of the noise spectrum  $S(\omega)$ .

Specifically, the noise spectrum of the system is quantum mechanically defined by the Fourier transform of the two-time particle correlation function:

$$S(\omega) = \lim_{t \rightarrow \infty} \int_{-\infty}^{\infty} e^{i\omega\tau} \langle a^\dagger(t + \tau) a(t) \rangle d\tau. \quad (11)$$

As we have shown recently [49], the two-time particle correlation function  $\langle a^\dagger(t + \tau) a(t) \rangle$  obeys the following relation in our exact master equation formalism,

$$\langle a^\dagger(t + \tau) a(t) \rangle = u^*(t + \tau) u(t) \langle a^\dagger(t_0) a(t_0) \rangle + v(t, t + \tau),$$

where

$$v(t, t + \tau) = \int_{t_0}^t d\tau_1 \int_{t_0}^{t+\tau} d\tau_2 u(t, \tau_1) \tilde{g}(\tau_1, \tau_2) u^*(t + \tau, \tau_2), \quad (12)$$

which is the more general form of Eq. (5). On the other hand, the exact analytic solution of the integro-differential equation (4) is also recently given in [53],

$$u(t) = \mathcal{Z} e^{-i\omega_b(t-t_0)} + \frac{1}{\pi} \int_0^\infty \frac{\gamma(\omega) e^{-i\omega(t-t_0)}}{[\omega - \omega_0 - \Delta(\omega)]^2 + \gamma^2(\omega)} d\omega, \quad (13)$$

where  $\gamma(\omega) = J(\omega)/2$  and  $\Delta(\omega) = \mathcal{P} \int_0^\infty \frac{J(\omega')}{\omega - \omega'} d\omega'$ , which are the real and imaginary parts of the self-energy correction,  $\Sigma(z)$ , to the resonator, induced by the coupling between the resonator and the environment,

$$\Sigma(z) = \int_0^\infty \frac{J(\omega)}{z - \omega} d\omega. \quad (14)$$

The first term in Eq. (13) is the contribution of the dissipationless localized mode, where the localized mode frequency  $\omega_b$  is determined by  $\omega_b - \omega_0 - \Delta(\omega_b) = 0$ , and  $\mathcal{Z} = [1 - \Sigma'(\omega_b)]^{-1}$  corresponds to the residue of  $\Sigma(z)$  at the pole  $z = \omega_b$ , which gives the amplitude of the localized mode.

Using the exact solution of Eq.(13) and the relation (12), we find that the noise spectrum is given by

$$\begin{aligned} S(\omega) &= \mathcal{Z}^2 \delta(\omega - \omega_b) \langle a^\dagger(t_0) a(t_0) \rangle + \left[ \frac{\mathcal{Z}^2 J(\omega)}{(\omega - \omega_b)^2} \right. \\ &\quad \left. + \frac{J(\omega)}{[\omega - \omega_0 - \Delta(\omega)]^2 + \gamma^2(\omega)} \right] \bar{n}(\omega, T) \\ &= S_1(\omega) + S_2(\omega), \end{aligned} \quad (15)$$

where  $S_1(\omega)$  and  $S_2(\omega)$  are the contributions of the particle correlations from the system and the environment respectively to the noise spectrum, due to the coupling between them. Now,  $S_2(\omega)$  can have a power series ex-

pansion with Legendre polynomials  $P_n(\xi)$  as

$$\begin{aligned}
 S_2(\omega) &= \frac{\mathcal{Z}^2 J(\omega) \bar{n}(\omega, T)}{(\omega - \omega_b)^2} + \frac{J(\omega) \bar{n}(\omega, T)}{\omega_0^2 + \gamma^2(\omega)} \left( \sum_{n=0} P_n(\xi) \zeta^n \right)^2 \\
 &= \frac{\mathcal{Z}^2 J(\omega) \bar{n}(\omega, T)}{(\omega - \omega_b)^2} + \frac{J(\omega) \bar{n}(\omega, T)}{\omega_0^2 + \gamma^2(\omega)} \left[ 1 + 2\xi\zeta \right. \\
 &\quad \left. + \mathcal{O}(\xi^2 \zeta^2) + \dots \right], \tag{16}
 \end{aligned}$$

where  $\xi = \omega_0 / \sqrt{\omega_0^2 + \gamma^2(\omega)}$ , and  $\zeta = (\omega - \Delta(\omega)) / \sqrt{\omega_0^2 + \gamma^2(\omega)}$ . We should only take the low-frequency limits  $\hbar\omega/k_B T \ll 1$  and  $\omega \ll \omega_0$ , in order to see the low frequency behavior of the noise spectrum. Through a numerical check, see figure 1(a), we find that for  $\eta \leq 10^{-3}$  and  $\omega/\omega_0 \leq 10^{-2}$ , one has  $\xi\zeta \ll 1$  and  $\omega_0^2 \gg \gamma^2(\omega)$ . Meanwhile, when the coupling between the system and the environment  $\eta \leq 10^{-3}$ , the localized mode amplitude ( $\mathcal{Z}$ ) becomes negligibly small, and therefore it does not play any role for low frequency behavior of the noise spectrum. Thus the noise spectrum is reduced to

$$S(\omega) = \frac{\eta' k_B T}{\omega^{1-s}} = \frac{\eta' k_B T}{\omega^x}, \tag{17}$$

where  $\eta' = \eta \omega_c^{1-s} / \hbar \omega_0^2$ . For  $s = 0$ , Eq.(17) gives the exact  $1/f$  noise spectrum. Generally, the low frequency noise ( $1/f^x$ ) dominates when  $x > 0$  or  $s < 1$  in the very weak coupling regime between the system and its reservoir. In figure 1(a), we show the range of  $\eta$  and  $\omega$  where the low frequency noise spectrum behaves as  $1/f^x$  power law. For  $x \approx 1$ , the  $1/f$  noise behavior shows up in the low frequency domain where the coupling strength  $\eta$  must be sufficiently weak. We also plot in figure 1(b) the noise spectrum  $S(\omega)$  for  $\eta = 10^{-3}$  with different values of  $x$ . Different  $1/f^x$  behaviors are displayed.

The above noise power spectrum, calculated analytically and exactly through the Fourier transform of the two-time particle correlation function (11), provides a fully quantum mechanical description of the  $1/f^x$  noise. This quantum mechanical description of the  $1/f$  noise shows that it valids in a very narrow range of  $\eta$  and  $\omega$  when both the frequency and the coupling strengths are very small, in comparison with the energy scale of the system.

#### IV. DECOHERENCE DYNAMICS UNDER $1/f^x$ NOISE

Now we shall study the exact decoherence dynamics induced by  $1/f$  noise under the condition  $\hbar\omega/k_B T \ll 1$  and  $\omega \ll \omega_0$ , and the dimensionless coupling strength  $\eta$  is sufficiently weak. We start with the  $1/f^x$  noise with  $x = 0.25$ , and gradually increase it to  $x = 0.5, 0.75$ , and  $0.9999$ , to examine the change of dissipation and fluctuation dynamics of the resonator when the noise spectrum

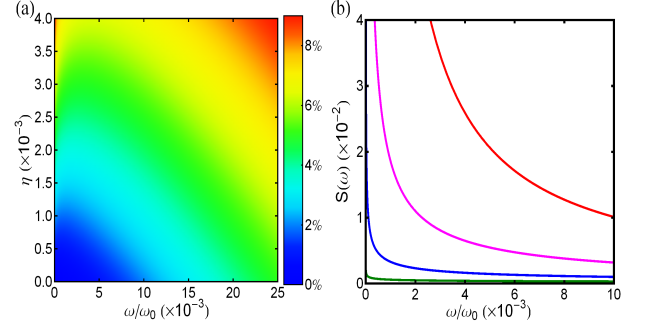


FIG. 1. (Color online) (a) We plot the first order correction term  $2\xi\zeta$  in the expansion of the noise spectrum (16) for  $\omega_c = \omega_0$ , which shows a very narrow range of  $\eta$  and  $\omega$  for the low frequency noise spectrum behaving as  $1/f^x$  power law. (b) The noise spectrum  $S(\omega)$  is plotted for different values of  $x$  as  $x = 0.25$  (green),  $x = 0.5$  (blue),  $x = 0.75$  (pink) and  $x = 0.9999$  (red) at  $\eta = 10^{-3}$  with  $\omega_c = \omega_0 = 5$  GHz, and  $T = 25$  mK.

approaches to  $1/f$ . Dissipation and fluctuation dynamics through the exact solution of  $u(t)$  and  $v(t)$  are presented in Figure 2 for  $1/f^x$  noise (10) with  $x = 0.25, 0.5, 0.75$ , and  $0.9999$ , respectively, corresponding to the four different curves in each graph. It shows how dissipation and fluctuation change as the reservoir spectra approach to low-frequency-dominated regime. One can see that for very weak coupling ( $\eta = 10^{-3}$ ), the particle propagating function  $u(t)$  has similar damping dynamics (monotonous decay) with different  $x$  values, see figure 2(a). We see similar decay dynamics for  $u(t)$  (without having any non-Markovian effect) even if we increase the coupling strength to  $\eta = 10^{-2}$  with changing  $x$  values, see figure 2(b). Figures 2(c) and (d) show thermal fluctuations in terms of the correlation Green's function  $v(t)$ . The correlation Green's function  $v(t)$  quantifies physically the thermal-fluctuation-induced average particle number inside the resonator, reflecting the noise effect of the decoherence dynamics. Figure 2(c) shows that the decoherence dynamics is significantly different for  $1/f$  spectrum ( $x = 0.9999$ ), as the oscillations of  $v(t)$  is very strong, compared to other  $1/f^x$  (with  $x = 0.25, 0.5, 0.75$ ) at weak coupling ( $\eta = 10^{-3}$ ). This is the signal of a non-Markovian decoherence dynamics purely induced by the noise effect. Physically this can be seen from Eq. (7) that the initial particle distribution function  $\bar{n}(\omega, T)$  induces explicitly frequency dependence to the memory kernel  $\tilde{g}(\tau - \tau')$ , and in particular, this frequency dependence becomes stronger in the low frequency regime  $\sim 1/\omega$ . This distinct oscillatory feature of  $v(t)$  persists even at higher coupling strength ( $\eta = 10^{-2}$ ), although it has a long time decay behavior, see figure 2(d). In conclusion, we show here, for the first time, the physical mechanism of non-Markovian dynamics induced by  $1/f$  noise even though the system-environment coupling is very small.

With the above exact solution of the dissipation and

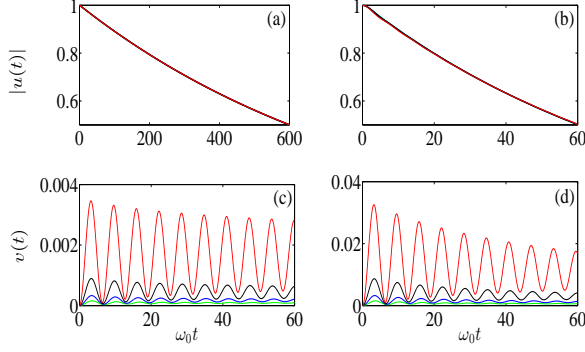


FIG. 2. (Color online) Comparison of the exact solution of  $|u(t)|$  and  $v(t)$  for  $1/f^x$  noise with  $x = 0.25$  (green),  $x = 0.5$  (blue),  $x = 0.75$  (black),  $x = 0.9999$  (red). We plot the exact  $|u(t)|$  and  $v(t)$  for different system-environment coupling  $\eta$ : (a,c)  $\eta = 10^{-3}$  and (b,d)  $\eta = 10^{-2}$ . The other parameters are taken as  $\omega_c = \omega_0 = 5$  GHz, and  $T = 25$  mK.

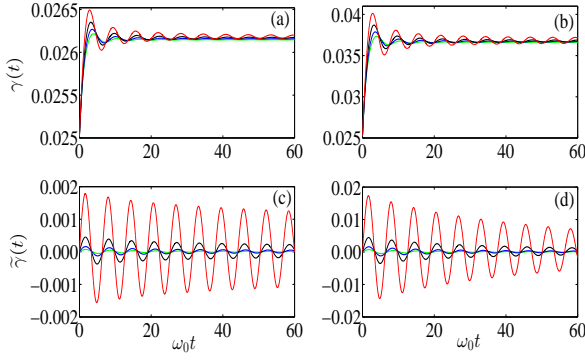


FIG. 3. (Color online) The dissipation and fluctuation coefficients  $\gamma(t)$  and  $\tilde{\gamma}(t)$  are calculated from the exact solution of  $u(t)$  and  $v(t)$  for  $1/f^x$  noise with  $x = 0.25$  (green),  $x = 0.5$  (blue),  $x = 0.75$  (black),  $x = 0.9999$  (red). We plot exact  $\gamma(t)$  for different system-environment coupling  $\eta$  (a)  $\eta = 10^{-3}$  and (b)  $\eta = 10^{-2}$ . We next plot exact  $\tilde{\gamma}(t)$  at (c)  $\eta = 10^{-3}$  and (d)  $\eta = 10^{-2}$ . The values of other parameters are  $\omega_c = \omega_0 = 5$  GHz, and  $T = 25$  mK.

fluctuation dynamics, we now present the dissipation and fluctuation coefficients in the master equation,  $\gamma(t)$  and  $\tilde{\gamma}(t)$ , which manifests quantitatively the decoherence behavior of  $1/f$  noise. Figures 3(a) and (b) show the time evolution of the dissipation coefficient  $\gamma(t)$  for different  $1/f^x$  noise with  $x = 0.25, 0.5, 0.75$ , and  $0.9999$  at two different values of the coupling strengths,  $\eta = 10^{-3}$  and  $10^{-2}$ , partnered to the solutions in figures 2(a) and (b). In the very weak coupling region ( $\eta = 10^{-3}$ ), including the  $1/f$  noise, we see from figure 3(a) that the dissipation coefficient  $\gamma(t) > 0$ , which indicates that the corresponding dissipation solution is always Markovian [54, 55]. A similar behavior of  $\gamma(t)$  with increased magnitude is seen when the coupling strength is increased ( $\eta = 10^{-2}$  for figure 3(b)). However, the fluctuation co-

efficient  $\tilde{\gamma}(t)$  is very sensitive to the noise spectrum and it behaves qualitatively different from the dissipation coefficient  $\gamma(t)$  in the weak-coupling regime, in particular, in the  $1/f$  noise regime. As one can see from figure 3(c),  $\tilde{\gamma}(t)$  oscillates between positive and negative values resulting to a non-Markovian memory effect. This positive and negative bounded value is significantly larger in case of  $1/f$  noise spectrum ( $x \sim 1$ ), compared to other spectrums with smaller values of  $x$ . The distinct oscillatory feature of  $\tilde{\gamma}(t)$  persists even at higher coupling strength ( $\eta = 10^{-2}$ ), with a long time decay behavior, see figure 3(d). The presence of this persistent oscillation between positive and negative values in fluctuation coefficient  $\tilde{\gamma}(t)$  but not in the dissipation coefficient  $\gamma(t)$ , shows the evidence for strong non-Markovian dynamics, associated with the  $1/f$  noise, as we have just pointed out in the analysis of the correlation Green's function  $v(t)$ . The decoherence dynamics of the resonator is very sensitive to the temperature for  $1/f^x$  spectrum. To show the effect of temperature dependence on the decoherence dynamics, we plot the non-equilibrium thermal fluctuation  $v(t)$  and the fluctuation coefficient  $\tilde{\gamma}(t)$  in figure 4 for  $1/f^x$  spectrum with  $x = 0.9999$  at various temperatures  $T = 25$  mK,  $T = 1.0$  K, and  $T = 2.5$  K, respectively. It shows that the magnitude of both  $v(t)$  and  $\tilde{\gamma}(t)$  becomes significant with the rising temperature even if the system-reservoir coupling is very small ( $\eta = 10^{-3}$ ). This temperature dependence comes through the particle number distribution  $\bar{n}(\omega, T)$  in Eq.(7), as purely a noise effect.

## V. DECOHERENCE DYNAMICS OF THE RESONATOR UNDER $1/f^x$ NOISE USING WIGNER DISTRIBUTION

Next, we explore the decoherence dynamics of quantum photon states under the  $1/f$  noise by examining the evolution of the corresponding Wigner function. With the help of the exact master equation (2), the exact Wigner function of an arbitrary quantum state at arbitrary time  $t$  in the complex space  $\{z\}$  is given by

$$W(z, t) = \int d\mu(\alpha_0) d\mu(\alpha'_0) \langle \alpha_0 | \rho(t_0) | \alpha'_0 \rangle \mathcal{T}(z, t | \alpha_0, \alpha'^*_0, t_0), \quad (18)$$

where  $|\alpha\rangle = e^{\alpha a^\dagger} |0\rangle$  is the coherent state,  $d\mu(\alpha) = \frac{d\alpha^* d\alpha}{2\pi i} e^{-|\alpha|^2}$  is the integral measure of the Bergman complex space,  $\rho(t_0)$  is the reduced density matrix of the initial state, and the propagating function  $\mathcal{T}(z, t | \alpha_0, \alpha'^*_0, t_0)$  is given by [52, 57]

$$\mathcal{T}(z, t | \alpha_0, \alpha'^*_0, t_0) = W_0^0(z, t) \exp \{ z^* \Omega(t) u(t) \alpha_0 + z \Omega(t) u^*(t) \alpha'^*_0 + \alpha'^*_0 [1 - |u(t)|^2 \Omega(t)] \alpha_0 \} \quad (19)$$

where

$$\Omega(t) = \frac{2}{1 + 2v(t)} \quad \text{and} \quad W_0^0(z, t) = \frac{2 \exp(-\Omega(t)|z|^2)}{\pi [1 + v(t)]}.$$

We investigate the damping and decoherence dynamics of the resonator in the presence of low frequency  $1/f^x$  noise at a finite temperature. We see the effect of changing values of  $x$  on the dynamics of the resonator which is prepared initially in a superposition of Fock states. If the resonator is initially prepared in a photon number superposition state  $\rho(t_0) = |\psi_0\rangle\langle\psi_0|$  with  $|\psi_0\rangle = 1/\sqrt{2}(|0\rangle + |n\rangle)$ . The time evolved Wigner function in this case is given by

$$W_0^n(z, t) = \frac{1}{2} [W_0^0(z, t) + W_n^n(z, t)] \quad (20)$$

$$+ \frac{W_0^0(z, t)}{2\sqrt{n!}} [(z\Omega(t)u^*(t))^n + (z^*\Omega(t)u(t))^n],$$

where  $W_0^0(z, t)$  is the time evolved Wigner function for the initial vacuum state, and

$$W_n^n(z, t) = W_0^0(z, t) \sum_{p=0}^n \frac{n!}{p!(n-p)!(n-p)!} \times \quad (21)$$

$$\left[ (|u(t)|^2 \Omega^2(t) |z|^2)^{n-p} (1 - |u(t)|^2 \Omega(t))^p \right].$$

The decoherence dynamics of the superposition state  $|\psi_0\rangle = 1/\sqrt{2}(|n\rangle + |m\rangle)$  can be examined through the time evolution of its Wigner function, given by

$$W_n^m(z, t) = \frac{1}{2} [W_n^n(z, t) + W_m^m(z, t)] \quad (22)$$

$$+ \frac{1}{2} W_0^0(z, t) \sum_{p=0}^{\min(n,m)} \frac{\sqrt{n!}\sqrt{m!}}{p!(n-p)!(m-p)!} \times$$

$$\{ (z^*\Omega(t)u(t))^{n-p} (z\Omega(t)u^*(t))^{m-p} (1 - |u(t)|^2 \Omega(t))^p +$$

$$(z^*\Omega(t)u(t))^{m-p} (z\Omega(t)u^*(t))^{n-p} (1 - |u(t)|^2 \Omega(t))^p \},$$

where  $W_m^m(z, t)$  is the same as  $W_n^n(z, t)$  with  $n$  being replaced by  $m$ . In figure 5, the time dependent snapshots of the Wigner functions are shown at four different times:  $\omega_0 t = 0, 1, 1.5, 2$ . Figure 5(a) describes the decoherence dynamics of the resonator in the presence of the low frequency  $1/f^x$  noise with  $x = 0.25$  at a finite temperature  $T = 2.5$  K, and the resonator is initially prepared in a superposition state  $1/\sqrt{2}(|0\rangle + |3\rangle)$ . The interference pattern consisting of three positive and three negative peaks are caused by the superposition between the states  $|0\rangle$  and  $|3\rangle$ . As time evolves, the off-diagonal elements of the density matrix decays with time and the positive and negative peaks disappear. In figure 5(b), we plot the time evolution of the Wigner function for the same superposition state  $1/\sqrt{2}(|0\rangle + |3\rangle)$  in presence of the  $1/f^x$  noise with  $x = 0.9999$ . We see distinct decoherence dynamics for the resonator initial state  $1/\sqrt{2}(|0\rangle + |3\rangle)$  under  $1/f^x$  noise with different “ $x$ ” values, where the decoherence rate is much faster for  $x = 0.9999$ . Next, we plot (figures 5(c) and (d)) the decoherence dynamics of the resonator state  $1/\sqrt{2}(|2\rangle + |3\rangle)$ , where the Wigner distribution functions show different decay dynamics of the interference fringe pattern due to the low frequency  $1/f^x$  noise (with  $x = 0.25$  and  $x = 0.9999$ ) of the bosonic

reservoir at finite temperature  $T = 2.5$  K. Faster decoherence dynamics is again observed as we increase the  $x$  value of the noise spectrum.

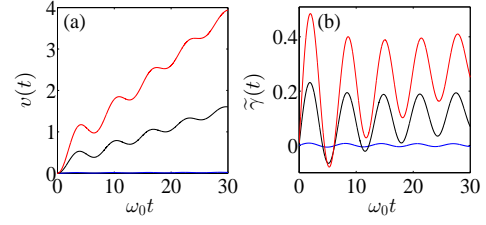


FIG. 4. (Color online) (a) the exact  $v(t)$  and (b) the fluctuation coefficient  $\tilde{\gamma}(t)$  (calculated from the exact solution of  $u(t)$  and  $v(t)$ ) for  $1/f$  spectrum with  $x = 0.9999$  at various temperatures  $T = 25$  mK (blue),  $T = 1.0$  K (black), and  $T = 2.5$  K (red). The other parameters are  $\eta = 10^{-3}$ , and  $\omega_c = \omega_0 = 1$  GHz.

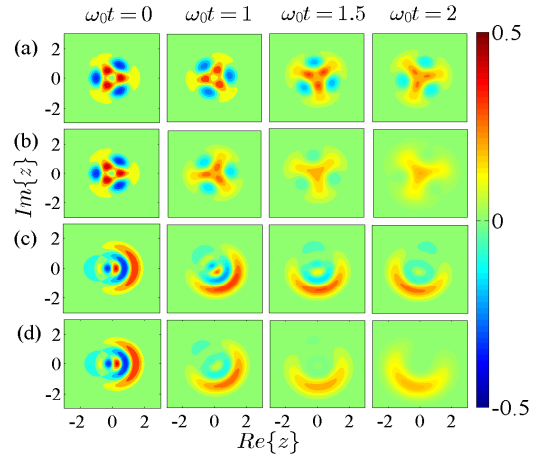


FIG. 5. (Color online) The decoherence dynamics of the resonator (prepared in initial superposition states  $1/\sqrt{2}(|0\rangle + |3\rangle)$  and  $1/\sqrt{2}(|2\rangle + |3\rangle)$ ) are respectively shown by plotting the time evolution of the Wigner function for  $1/f^x$  noise with (a) and (c) with  $x = 0.25$ , and also (b) and (d) with  $x = 0.9999$ . The values of other parameters are  $\eta = 10^{-3}$ ,  $\omega_c = \omega_0 = 1$  GHz, and  $T = 2.5$  K.

## VI. CONCLUSION

In conclusion, the exact decoherence dynamics of a quantum resonator coupled to a low frequency bosonic reservoir is explored. The noise power spectrum is calculated analytically and exactly using the exact solutions of the nonequilibrium Green's functions. It is found that the  $1/f^x$  power law behavior of the noise spectrum is valid for a very narrow range of  $\eta$  and  $\omega$  when both the frequency and the coupling strengths are very small, in



comparison with the energy scale of the system. The non-Markovian dynamics of the resonator in the weak coupling regime is produced by the noise effect. The correlation Green's function  $v(t)$  and hence the fluctuation coefficient  $\tilde{\gamma}(t)$  shows a long-time non-Markovian oscillatory behavior which is qualitatively different from the Markovian dissipation dynamics described by the propagating Green's function  $u(t)$  and the dissipation coefficient  $\gamma(t)$  in the ultra-weak coupling regime, in particular, in the  $1/f$  regime. We have shown through the exact master equation the evolution of a number of nonclassical photon states of the resonator in the presence of  $1/f$  noise, where the finite temperature effect of the bosonic reservoir is also examined. The faster decoherence behavior due to the  $1/f^x$  noise is demonstrated by increasing the  $x$  value. Our analysis is also applicable to another

nano/micro mechanical oscillators, and we believe that the results presented here can enhance the understanding of non-Markovian decoherence dynamics for many solid state quantum devices in the *very weak* system-reservoir coupling regime, when the  $1/f$  noise is dominated.

## ACKNOWLEDGMENTS

This work is supported by the National Science Council of ROC under Contract No. NSC-102-2112-M-006-016-MY3 and The National Center for Theoretical Sciences. It is also supported in part by the Headquarters of University Advancement at the National Cheng Kung University, which is sponsored by the Ministry of Education, Taiwan, ROC.

- 
- [1] I. Flinn, *Nature* **219**, 1356 (1968).
  - [2] R. F. Voss and J. Clarke, *Nature* **258**, 317 (1975).
  - [3] D. L. Gilden, T. Thornton and M. W. Mallon, *Science* **267**, 1837 (1995).
  - [4] R. J. Schoelkopf, P. Wahlgren, A. A. Kozhevnikov, P. Delsing, and D. E. Prober, *Science* **280**, 1238 (1998).
  - [5] E. Simoen and C. Claeys, *Solid State Electron* **43**, 865 (1999).
  - [6] A. A. Balandin, *Noise and Fluctuations Control Electronic Devices* (American Scientific, California, 2002).
  - [7] R. Pettai, *Noise in Receiving Systems* (Wiley, New York, 1984).
  - [8] C. D. Motchenbacher and F. C. Fitchen, *Low-Noise Electronic Design* (Wiley, New York, 1973).
  - [9] P. Dutta and P. M. Horn, *Rev. Mod. Phys.* **53**, 497 (1981).
  - [10] M. B. Weissman, *Rev. Mod. Phys.* **60**, 537 (1988).
  - [11] E. Paladino, Y. M. Galperin, G. Falci, and B. L. Altshuler, *Rev. Mod. Phys.* **86**, 361 (2014).
  - [12] A. B. Zorin, F.-J. Ahlers, J. Niemeyer, T. Weimann, H. Wolf, V. A. Krupenin, and S. V. Lotkhov, *Phys. Rev. B* **53**, 13682 (1996).
  - [13] V. A. Krupenin, D. E. Presnov, M. N. Savvateev, H. Scherer, A. B. Zorin and J. Niemeyer, *J. Appl. Phys.* **84**, 3212 (1998).
  - [14] M. Kenyon, C. J. Lobb and F. C. Wellstood, *J. Appl. Phys.* **88**, 6536 (2000).
  - [15] T. F. Li, Y. A. Pashkin, O. Astafiev, Y. Nakamura, J. S. Tsai, and H. Im, *Appl. Phys. Lett.* **91**, 033107 (2007).
  - [16] G. Liu, W. Stillman, S. Rumyantsev, Q. Shao, M. Shur, and A. A. Balandin, *Appl. Phys. Lett.* **95**, 033103 (2009).
  - [17] Y. Nakamura, Y. A. Pashkin, T. Yamamoto, and J. S. Tsai, *Phys. Rev. Lett.* **88**, 047901 (2002).
  - [18] O. Astafiev, Y. A. Pashkin, Y. Nakamura, T. Yamamoto, and J. S. Tsai, *Phys. Rev. Lett.* **96**, 137001 (2006).
  - [19] F. Yoshihara, K. Harrabi, A. O. Niskanen, Y. Nakamura, and J. S. Tsai, *Phys. Rev. Lett.* **97**, 167001 (2006).
  - [20] K. Kakuyanagi, T. Meno, S. Saito, H. Nakano, K. Semba, H. Takayanagi, F. Deppe, and A. Shnirman, *Phys. Rev. Lett.* **98**, 047004 (2007).
  - [21] R. H. Koch, D. P. DiVincenzo, and J. Clarke, *Phys. Rev. Lett.* **98**, 267003 (2007).
  - [22] J. Q. You and F. Nori, *Nature* **474**, 590 (2011).
  - [23] Z.-L. Xiang, S. Ashhab, J. Q. You and F. Nori, *Rev. Mod. Phys.* **85**, 623 (2013).
  - [24] S. M. Anton et al., *Phys. Rev. B* **85**, 224505 (2012).
  - [25] M. Niemann, H. Kantz and E. Barkai, *Phys. Rev. Lett.* **110**, 140603 (2013).
  - [26] L. Tian, *Phys. Rev. Lett.* **98**, 153602 (2007).
  - [27] R. C. Bialczak, R. McDermott, M. Ansmann, M. Hofheinz, N. Katz, E. Lucero, M. Neeley, A. D. O'Connell, H. Wang, A. N. Cleland, and J. M. Martinis, *Phys. Rev. Lett.* **99**, 187006 (2007).
  - [28] J. Bylander, S. Gustavsson, F. Yan, F. Yoshihara, K. Harrabi, G. Fitch, D. G. Cory, Y. Nakamura, J.-S. Tsai and W. D. Oliver, *Nature Phys.* **7**, 565 (2011).
  - [29] D. Sank, R. Barends, R. C. Bialczak, Y. Chen, J. Kelly, M. Lenander, E. Lucero, M. Mariantoni, A. Megrant, M. Neeley, P. J. J. O'Malley, A. Vainsencher, H. Wang, J. Wenner, T. C. White, T. Yamamoto, Y. Yin, A. N. Cleland, and J. M. Martinis, *Phys. Rev. Lett.* **109**, 067001 (2012).
  - [30] S. M. Anton, C. Müller, J. S. Birenbaum, S. R. O'Kelley, A. D. Fefferman, D. S. Golubev, G. C. Hilton, H.-M. Cho, K. D. Irwin, F. C. Wellstood, G. Schön, A. Shnirman, and J. Clarke, *Phys. Rev. B* **85**, 224505 (2012).
  - [31] C. Benedetti, F. Buscemi, P. Bordone, and M. G. A. Paris, *Phys. Rev. A* **87**, 052328 (2013).
  - [32] C. Benedetti, M. G. A. Paris, and S. Maniscalco, *Phys. Rev. A* **89**, 012114 (2014).
  - [33] E. Paladino, L. Faoro, G. Falci, and R. Fazio, *Phys. Rev. Lett.* **88**, 228304 (2002).
  - [34] G. Falci, A. D. Arrigo, A. Mastellone, and E. Paladino, *Phys. Rev. Lett.* **94**, 167002 (2005).
  - [35] Y. M. Galperin, B. L. Altshuler, J. Bergli, and D. V. Shantsev, *Phys. Rev. Lett.* **96**, 097009 (2006).
  - [36] J. Bergli, Y. M. Galperin, and B. L. Altshuler, *New J. Phys.* **11**, 025002 (2009).
  - [37] A. Ourjoumtsev, H. Jeong, R. T. Bouri and P. Grangier, *Nature* **448**, 784 (2007).
  - [38] S. Deléglise, I. Dotsenko, C. Sayrin, J. Bernu, M. Brune, J. M. Raimond and S. Haroche, *Nature* **455**, 510 (2008).
  - [39] H. Wang, M. Hofheinz, M. Ansmann, R. C. Bialczak, E. Lucero, M. Neeley, A. D. O'Connell, D. Sank, M. Weides,

- J. Wenner, A. N. Cleland, and J. M. Martinis, Phys. Rev. Lett. **103**, 200404 (2009).
- [40] J. Gao, J. Zmuidzinas, B. A. Mazin, H. G. LeDuc, and P. K. Day, Appl. Phys. Lett. **90**, 102507 (2007).
- [41] K. W. Murch, S. J. Weber, E. M. L. Falk, R. Vijay, and I. Siddiqi, Appl. Phys. Lett. **100**, 142601 (2012).
- [42] X. L. Feng, C. J. White, A. Hajimiri and M. L. Roukes, Nature Nanotech **3**, 342 (2008).
- [43] J. M. Gray, K. A. Bertness, N. A. Sanford, and C. T. Rogers, Appl. Phys. Lett. **101**, 233115 (2012).
- [44] R. P. Feynman and F. L. Vernon, Ann. Phys. (NY) **24**, 118 (1963).
- [45] A. O. Caldeira and A. J. Leggett, Physica A **121**, 587 (1983).
- [46] A. J. Leggett, S. Chakravarty, A. T. Dorsey, M. P. A. Fisher, A. Garg, and W. Zwerger, Rev. Mod. Phys. **59**, 1 (1987).
- [47] F. Haake and R. Reibold, Phys. Rev. A **32**, 2462 (1985).
- [48] W.-M. Zhang, D. H. feng and R. Gilmore, Rev. Mod. Phys. **62**, 867 (1990).
- [49] C. U. Lei and W.-M. Zhang, Ann. Phys. **327**, 1408 (2012).
- [50] H.-N. Xiong, W.-M. Zhang, X. Wang, and M.-H. Wu, Phys. Rev. A **82**, 012105 (2010).
- [51] H.-T. Tan and W.-M. Zhang, Phys. Rev. A **83**, 032102 (2011).
- [52] C. U. Lei and W.-M. Zhang, Phys. Rev. A **84**, 052116 (2011). Note that typos in the solution of  $\Omega(t)$  and  $W_0^0(z, t)$  after Eq. (7) in that paper are corrected here, and also see [57].
- [53] W.-M. Zhang, P.-Y. Lo, H.-N. Xiong, M. W.-Y. Tu, and F. Nori, Phys. Rev. Lett. **109**, 170402 (2012).
- [54] D. Chruściński and A. Kossakowski, Phys. Rev. Lett. **104**, 070406 (2010).
- [55] D. Chruściński and A. Kossakowski, and A. Rivas, Phys. Rev. A **83**, 052128 (2011).
- [56] A. Shnirman, Y. Makhlin, and G. Schön, Phys. Scr. **T102**, 147 (2002).
- [57] A. Rançon and J. Bonart, Euro. Phys. Lett. **104**, 50010 (2013).